NEAR-FIELD OPTICS

Light on the Nanoworld

Dieter Pohl from the IBM's Zurich Research Laboratory, Rüschlikon, explains why imaging and spectroscopy techniques based on scanning near-field optical microscopy are generating so much interest.

The wealth of optical phenomena offers numerous opportunities for interaction with the world of mesoscopic dimensions if one succeeds in confining the optical excitation to a correspondingly small volume. The optical effects then manifest themselves in novel ways similar to those found in waveguides and microwave antennae. Scanning near-field optical microscopy (SNOM) is based on this principle. The technique requires material structures that themselves have nanometre-sized dimensions. Small apertures, small particles acting as scattering centres, pointed glass fibres, or metallic tips, including the micromechanical tips used in atomic force microscopy, are suitable. When appropriately integrated into a scanning probe microscope, these structures can provide optical scan images with a resolution in the 10-100 nm range; these images are not diffraction-limited.

SNOM has recently became the focus of considerable scientific and technical interest because it is the only scanning probe microscopy that has well-understood material specificity (colour, polarization, fluorescence). The field is expanding rapidly so it is useful to give a brief overview of the state-of-the-art and the most frequently used techniques, as illustrated by some recent results from IBM Rüschlikon and the ETH Zurich.

a-SNOM (aperture near-field)

The most popular SNOM to date is aperture- (a-) SNOM [1], sometimes called NSOM where the "N" stands for "normal". Based on a probe design developed at IBM some 10 years ago, its essential component is a pointed, transparent tip coated with an opaque metal film such that a small aperture is formed at the apex of the tip (Figs 1a-c). In the early days, these tips were made of etched quartz crystals. Currently, the tips of choice are optical fibres pulled or etched to form a sharp point. The transparent micromechanical cantilever tips that have been introduced recently as SNOM probes constitute a promising new alternative.

The conical screen formed by the metallic coating of the tip is a waveguide which is overdamped near the apex. Its transmission decreases strongly as the diameter shrinks. a-SNOM is therefore limited to aperture diameters of about 30 to 70 nm and provides a resolution of approximately the same magnitude. Novel waveguide geometries which do not exhibit a cut-off (*e.g.*, coaxial cones or slotted-wall structures) might provide higher transmission volumes, thereby possibly allowing the resolution to be improved.

An aperture-SNOM is usually operated in the emission mode (Fig. 1a), meaning that light is focused into the optical probe from the far end. A tiny amount of radiation is transmitted by the aperture, interacts with the object in front of it, and is collected by focusing optics (*e.g.*, an auxiliary conventional optical microscope). The collection mode (Fig. 1b) is less frequently used, mainly because more intense exposures are needed. The reflection mode (Fig. 1c), first demonstrated in 1988, has recently attracted increasing attention. The gap width between the probe and object is usually controlled by an auxiliary distance-sensing mechanism (generally by monitoring the onset of electrical or mechanical contact). A topographic image of the object is therefore normally obtained together with the near-field optical images.

STOM (scanning tunnelling)

A second popular implementation of near-field optics is called scanning tunnelling optical microscopy (STOM) or photon tunnelling scanning microscopy (PSTM) [2]. The STOM/PSTM method is based on tapping an evanescent surface wave by means of an uncoated transparent tip, *i.e.*, by using the "tunnelling" of photons. The evanescent wave is created by total internal reflection at the surface of a prismatically or hemispherically shaped support for the object. The principle of operation is closely analogous to that of an electron scanning tunnelling microscope. In particular, the signal as a function of the gap-width has a distinct exponential form, in contrast to the standard a-SNOM. A STOM probe is easily prepared and the imaging capabilities of a STOM device are comparable to those of a-SNOM, although less well understood. It is possible to invert the light path to reduce exposure of the object during imaging.

TNOM (tunnelling near field)

A SNOM-type microscope that combines the advantages of both a-SNOM (a well-defined interaction volume) and STOM (a well-defined gap dependence) is the "forbidden light" or tunnelling near-field optical microscope (TNOM; see Fig. 2) [3]. It employs the usual aperture tip but detects both the light coupled *via* evanescent wave photon tunnelling and the forward-transmitted light (the standard, or "allowed" a-SNOM mode). The forbidden contribu-

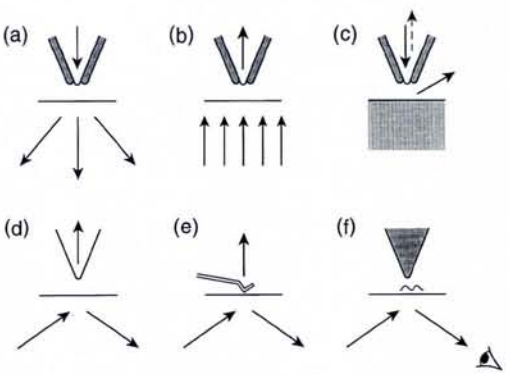

Fig. 1 - Various types of probes used for near-field optics. *A; upper) aperture probes operated in transmission (a), collection (b) and reflection (c) modes. B; lower) scanning tunnelling optical microscopy (STOM/PSTM) using a fibre tip (d), an atomic force microscope tip (e) and a scanning tunnelling microscope tip (f). Arrows indicate the flow of light; opaque components are in grey. The optical probe descends from above onto the horizontal surface of the object (given by the horizontal line).*

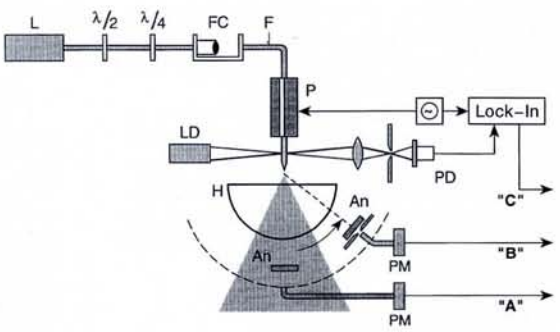

Fig. 2 - Experimental arrangement for a tunnelling near-field optical microscope (TNOM) combining a-SNOM and STOM. *Light from a laser (L) passes through a combination of 1/2-wave and 1/4-wave plates for polarization adjustment, and via a fibre coupler (FC) into a monomode optical fibre (F) with a pointed end acting as an optical probe. The fibre is mounted on a piezo-actuator. A shear force detection system for topographic imaging (friction force; output channel "C") is based on lateral vibrations of the tip. The vibration modulates the intensity of the light from a laser diode (LD) impinging on a detector (PD). Allowed light (shaded triangle; channel "A") and forbidden light (dotted line; channel "B") are detected using polarization analyzers (An) and photomultipliers (PM). The sample is mounted on a hemispherical (H) support.*

Dieter W. Pohl is a Research Staff Member at the IBM Research Division, Zurich Research Laboratory, CH-8803 Rüschlikon.

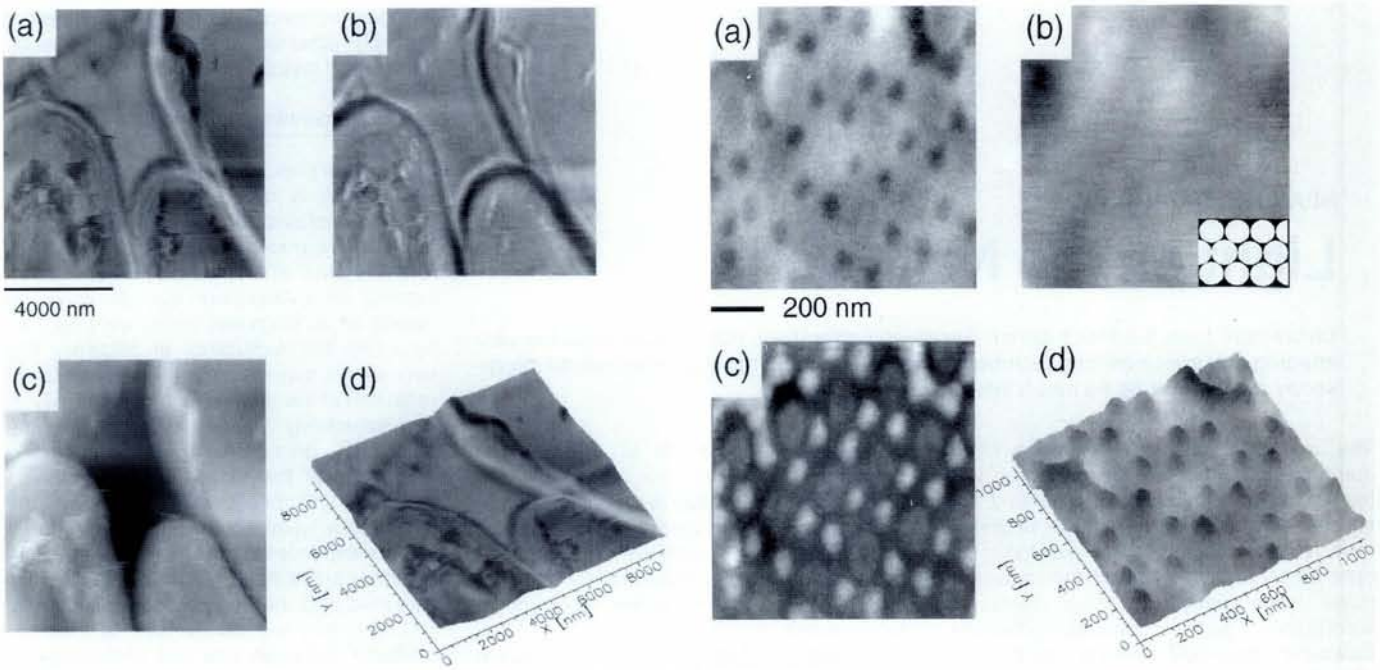

Fig. 3 - Examples of near-field optical imaging
A; left) phase-contrast imaging: red blood cells on a glass substrate showing their characteristic ellipsoidal shape (air dried; observed under green light). Many features appear with reversed contrast in forbidden (a) and allowed (b) light. This behaviour is typical for transparent objects (phase contrast); it allows one to distinguish them from absorbing objects (amplitude contrast). The two optical images reveal various details smaller than 100 nm in size that are not resolved in the topographic (friction) image (c) obtained simultaneously. Image (d) gives a three-dimensional superimposition of (a) and (c).
B; right) amplitude-contrast imaging: glass plate with a metallic pattern obtained by using an array of latex spheres to cast shadows during vapour deposition (sample prepared by U.Ch. Fischer, University of Münster). The array of uncoated spherical areas is illustrated in the inset of (b). The images demonstrate the immunity of forbidden light imaging to a background of stray light. The metallic patches (Al; thickness 15 nm; lateral extension approx. 50 nm) appear as a dark-contrasting regular pattern in the "forbidden" image (a). Some patches have a triangular shape, indicating that the resolution exceeds 50 nm. The "allowed" image (b) is partly obscured by stray light coming from imperfections at the sidewall of the optical probe, a shortcoming that sometimes occurs during the production of optical tips. The topographic (friction) image is shown in (c). (d) is a three-dimensional superimposition of (a) and (c).
All images from [4], with permission.

tions are transmitted at angles larger than a critical one and cannot therefore be detected with a standard a-SNOM.

Applications of TNOM

Fig. 3 is a series of recent TNOM images to illustrate the current level of imaging performance. The TNOM geometry is well suited for the spectroscopy of individual molecules [5, 6] — a capability that offers some of SNOM's most intriguing possibilities. To perform spectroscopy it is necessary to replace the detectors shown in Fig. 2 with an elliptical or parabolical mirror to allow a large proportion of the total fluorescence intensity to be collected. The decomposition of an inhomogeneous excitation spectrum into contributions from individual molecules allows, for instance, molecules to be identified by their saturation behaviour and Stark shift (Fig. 4).

Major applications are to be expected in biological research (high-resolution localization of fluorescent markers) and in microelectronics. Other applications include magnetic domain imaging on the basis of the magneto-optic Kerr effect and photophysical processing on the nanometre scale.

Theoretical Aspects

The ability to separate the source, the zone of interaction and the detector, while permitting different modes of SNOM operation, tends to complicate the understanding of near-field phenomena. Near- and far-field effects have to be considered simultaneously, a problem that cannot be handled using the theoretical tools of classical optics or electrostatics. As a result, questions dealing with aspects such as resolution and contrast limits have so far been left mainly to heuristic arguments and experimental evidence.

The modelling of light propagation through the complicated SNOM geometry requires the numerical solution of Helmholtz equations. Several specific configurations have recently been studied to give some insight into the optical properties of the SNOM geometry. As an example, Fig. 5A shows the calculated electrical energy density (electric field squared) for a two-dimensional a-SNOM (*i.e.*, for a slit aperture as opposed to a circular aperture). One clearly sees how a small metallic object severely disturbs the flow of radiation from the slit to the far field where the detector would be located.

First results for three-dimensional models indicate a similar behaviour. For instance, Fig. 5B shows the three-dimensional field distribution for an aluminium-coated glass-fibre probe. Note the strong decay of light intensity in the conical part of the optical probe (as discussed above), which constitutes a major limitation with regard to increasing the resolution by reducing the aperture size.

Scanning near-field optical microscopy is clearly more complex than other scanning probe techniques, but it provides a much wider variety of information. It has the advantage of not being limited by diffraction so it readily yields a resolution of 30 to 70 nm for both amplitude and phase objects. Aperture-SNOM having a resolution 30 nm

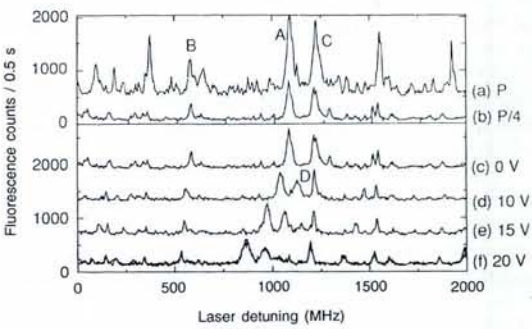

Fig. 4 - Statistical fine structure and single-molecule features
[6]. The excitation spectrum (fluorescence intensity versus laser detuning) of a pentacene-doped p-terphenyl sample obtained using near-field optical techniques. Upper panel: spectra taken with a 100 mW (curve a) and 25 mW (curve b) pumped laser power indicate the onset of saturation of some of the absorption lines. Lower: increasingly larger voltages (0-20 V) applied to the metallic coating of the optical fibre probe causes a Stark shift of some lines.

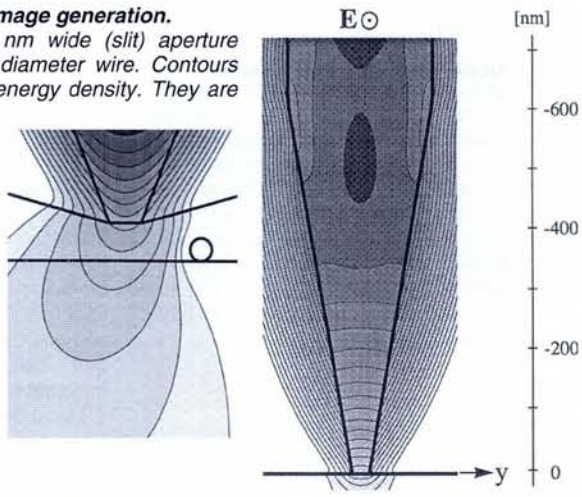

Fig. 5 - Modelling of SNOM image generation. *A; left) two-dimensional, 30 nm wide (slit) aperture scanned across a 20 nm in diameter wire. Contours give the calculated electrical energy density. They are severely disturbed when the object passes across the slit. From [7].*
B; right) three-dimensional, aluminium-coated pointed glass-fibre tip. Contours giving the calculated flux of light along the path to the tip apex show a strong decrease in intensity on approaching the apex (x-direction parallel to the plane of polarization; factor of three between successive contour lines).

for both amplitude and phase contrast has reached a reasonably advanced level of maturity. But to achieve its ultimate resolution, possibly in the 1-3 nm range, it will be necessary to invent new near-field optical probes differing considerably from the ones employed up to now.

ACKNOWLEDGMENTS

The development of "forbidden light" microscopy at IBM Rüschlikon is the result of an extensive collaboration between experimentalists and theoreticians. The author should like to thank, in particular, A. Dereux, B Hecht, H. Heinzelmann, and L. Novotny for their dedicated work and essential contributions.

FURTHER READING & REFERENCES

Pohl D.W., in *Scanning Tunneling Microscopy II* (Springer Series in Surface Science), Eds.: R. Wiesendanger & H.J. Güntherodt (Springer-Verlag, 1992) p. 233.
Betzig E. & Trautman J., *Science* **257** (1992) 189.
van Hulst N.F., Moers M.H.P. & Bölger B., *J. Microscopy* **171** (1993) 95.
Heinzelmann H. & Pohl D.W., *Appl. Phys. A* **59** (1994) 89.
[1] Pohl D.W., Denk W., & Lanz M, *Appl. Phys. Lett.* **44** (1984) 651; Dürig U., Pohl D.W. & Rohner F., *J. Appl. Phys.* **59** (1986) 3318; Harootunian A. *et al.*, *Appl. Phys. Lett.* **49** (1986) 674; Betzig E., Isaacson M. & Lewis A., *App. Phys. Lett.* **51** (1987) 2088.
[2] Courjon D., Sarayeddine K. & Spajer M., *Optics Commun.* **71** (1989) 23; Reddick R.C. *et al.*, *Phys. Rev. B* **39** (1989) 767; de Fornel F. *et al.*, *Proc. SPIE* **1139** (1994) 2927.
[3] Hecht B., Heizelmann H. & Pohl D.W., *Ultramicroscopy* **57** (1995) 228.
[4] Hecht B., Pohl D.W, Heizelmann H. & Novotony L., in *Photons & Local Probes*; NATO ASI Series E: Applied Sciences. Eds: O. Marti & R. Möller (Kluwer; in press).
[5] Trautmann J.K. *et al.*, *Nature* **369** (1994) 40; Xie X.S & Dunn R.C., *Science* **265** (1994), 361; Ambrose W.P. *et al.*, *ibid.*, 364.
[6] Moerner W.E. *et al.*, *Phys. Rev. Lett.* **73** (1994) 2764.
[7] Novotny L., Pohl D.W. & Regli P., *J. Opt. Soc. Amer. A* **11** (1994) 1768.

BOSE-EINSTEIN CONDENSATION

A Fascinating Period Lies Ahead

J.T.M. Walraven from the Van der Waals - Zeeman Institute, Amsterdam University, discusses the implications of recent observations of Bose-Einstein condensation in alkali metal gases.

A very exciting recent experiment by Eric Cornell and Carl Wieman at JILA (Boulder, CO, USA) marks the beginning of a new chapter in the history of degenerate quantum systems. In early June, the JILA group observed Bose-Einstein condensation (BEC) in an ultra-cold gas of ^{87}Rb atoms, and started the first experiments on a degenerate atomic Bose gas [see M.H. Anderson M.H. *et al.*, *Science* **269** (1995) 198]. More recently, BEC has been announced for ^{7}Li by Randall Hulet at Rice University, USA. Other systems are likely to follow in the near future.

Unlike liquid helium, the only degenerate boson fluid thus far investigated, the dilute Bose gases are weakly interacting. This allows for large condensate fractions and an exceptionally transparent physical picture of many-body quantum behaviour. Not surprisingly, the quantum gases have intrigued and inspired physicists throughout this century. In the absence of experimental examples, their importance as theoretical model systems gave rise to a whole literature on "fictitious" ideal or nearly ideal degenerate quantum gases, both Bose and Fermi systems. In these studies, the dilute boson gas was invaluable for the development of the microscopic theory of superfluidity, starting from first principles with the binary collision approximation at temperatures where only s-wave scattering is assumed to contribute.

An image of the velocity distribution of a cloud of cooled and trapped Rb atoms that have formed a Bose-Einstein condensate. The high-density central (light contrasting) region is elliptical indicating that it has a highly nonthermal distribution (it is in fact an image of a single macroscopically occupied quantum wave function). Andersen M.H. et al., Science ***269*** *(1995) 199, with permission*

Search Culminated

The recent experiment at JILA forms the culmination point of a research programme in which two important principles from earlier experiments with ultra-cold atomic gases were successfully combined, namely (a) trapping by laser cooling methods with optical investigation of the samples, and (b) evaporative cooling of magnetically trapped samples to achieve BEC. Laser cooling proved extremely powerful to trap a variety of ultra-cold atoms with easily accessible optical transitions, in particular alkali atoms. Sensitive and convenient optical detection methods were developed, capable of imaging even a small number of atoms. However, optical cooling methods appear to be less suited to obtaining BEC because several light-related phenomena tend to limit achievable densities and temperatures to values far from those required for BEC. Evaporative cooling involves the preferential removal of the most energetic atoms from a sample and was developed with the aim of achieving BEC in spin-polarized atomic hydrogen, the first quantum gas to be studied experimentally. Although many properties of non-degenerate quantum gases have been investigated with hydrogen, in this system the progress towards BEC is slowed down by the lack of good diagnostics.

Exciting Prospects

There are several aspects that make the JILA experiment significant beyond the mere observation of BEC. Unlike liquid helium, the trapped atomic gases are inhomogeneous. This gives rise to an unique and almost complete spatial separation between the condensate and above-condensate particles. The separation manifests itself in one of the most exciting features of the JILA experiment. Once the condensate has formed, the above-condensate particles can be removed "mechanically" using a radiofrequency-based technique, enabling almost instant cooling to immeasurably low temperatures and leaving an essentially pure condensate which could be observed for about 15 s. The inhomogeneity also allows the investigation of interaction-related phenomena in spite of the fact that the samples are extremely